

Enhanced Zeeman splitting in $\text{Ga}_{0.25}\text{In}_{0.75}\text{As}$ quantum point contacts

T. P. Martin,^{*} A. Szorkovszky, A. P. Micolich, and A. R. Hamilton

School of Physics, University of New South Wales, Sydney NSW 2052, Australia

C. A. Marlow, H. Linke, and R. P. Taylor[†]

Department of Physics, University of Oregon, Eugene OR 97403, USA

L. Samuelson

Division of Solid State Physics, Lund University, Box 118, S-221 00 Lund, Sweden

(Dated: October 23, 2018)

Abstract

The strength of the Zeeman splitting induced by an applied magnetic field is an important factor for the realization of spin-resolved transport in mesoscopic devices. We measure the Zeeman splitting for a quantum point contact etched into a $\text{Ga}_{0.25}\text{In}_{0.75}\text{As}$ quantum well, with the field oriented parallel to the transport direction. We observe an enhancement of the Landé g -factor from $|g^*| = 3.8 \pm 0.2$ for the third subband to $|g^*| = 5.8 \pm 0.6$ for the first subband, six times larger than in GaAs. We report subband spacings in excess of 10 meV, which facilitates quantum transport at higher temperatures.

PACS numbers: 73.21.Hb, 71.70.Ej, 85.75.-d

The control of a charge carrier's spin is typically achieved using an applied magnetic field, and provides an extra degree of freedom that can be utilized for device functionalities such as spintronics, quantum information, etc.^{1,2,3,4} In semiconductor devices, the field B breaks the degeneracy of the two spin states via the Zeeman effect, resulting in spin-polarized transport, where a particular spin orientation dominates the electrical conductance of the device.^{1,2} The Zeeman spin-splitting is given by $\Delta E_z = g^* \mu_B B$, where g^* is the effective Landé g -factor and μ_B is the Bohr magneton. Since the strength of the spin-splitting is governed by g^* , narrow band-gap materials with a large g -factor such as GaInAs or InAs are highly desirable in the quest to develop electronic devices that require only the smallest magnetic fields to achieve spin-functional operations.

The small band-gap in the $\text{Ga}_x\text{In}_{1-x}\text{As}$ material system makes a large g -factor possible due to mixing of the conduction band electron states with valence band states. For example, in GaInAs quantum wells, g -factors ranging from 2.9 to 4.4 have been measured^{5,6,7,8} – an order of magnitude larger than in equivalent GaAs quantum wells.^{6,9} It is thus interesting to know how the g -factor in lower-dimensional structures will behave, because the additional confinement alters the coupling between the conduction and valence bands. In both n -type and p -type GaAs quantum point contacts (QPCs), the confinement of electrons to a quasi-one-dimensional (quasi-1D) system can lead to an enhancement of $|g^*|$ by as much as a factor of two over its 2D value, with the enhancement increasing as the 1D confinement is strengthened.^{10,11,12,13} Unexpectedly, the only measurement to date of the g -factor in a GaInAs QPC⁸ gave $|g^*| \approx 4$ in the 1D limit, showing no clear enhancement over the value of $|g^*|$ obtained in the 2D reservoirs adjacent to the QPC.⁸

In this letter, we use parallel field measurements (oriented in the plane of the quantum well along the QPC) to study how the strength of the 1D confinement affects the spin-splitting in an etched $\text{Ga}_{0.25}\text{In}_{0.75}\text{As}$ QPC. In contrast to the measurements obtained using perpendicular fields by Schäpers *et al.*,⁸ we observe a clear enhancement of the g -factor in the 1D limit of our device. Our result is consistent with the 1D enhancement observed in GaAs QPCs, which was also measured using parallel field techniques.^{10,11,12,13} The key difference between our measurements and those of Reference 8 is the field direction, and we use this to explain why 1D g -factor enhancement was not observed in their study.

Our QPC is etched into a GaInAs/InP modulation-doped heterostructure, where a 2D electron gas (2DEG) is confined to a 9 nm thick $\text{Ga}_{0.25}\text{In}_{0.75}\text{As}$ quantum well.^{14,15} The

QPC investigated is ~ 160 nm long and ~ 120 nm wide, and fabricated on a Hall bar mesa featuring NiGeAu Ohmic contacts. A Ti/Au top-gate, deposited uniformly over the mesa, is used to tune the Fermi energy E_F and thus change the number of occupied subbands n in the QPC. All measurements were performed in a ^4He cryostat with a base temperature of 1.3 K. Standard four-probe and lock-in amplification techniques were used to measure the differential conductance $G = dI/dV$ through the QPC at a frequency of 17 Hz and constant excitation voltage of $100 \mu\text{V}$ ($300 \mu\text{V}$ for source-drain biasing). The 2D carrier density and mobility were $5.6\text{--}6.8 \times 10^{11} \text{ cm}^{-2}$ and $1.3\text{--}2.2 \times 10^5 \text{ cm}^2/\text{Vs}$ respectively within the range of applied gate voltages presented here (-6.0 to 1.5 V). Our 2D density and mobility, gallium fraction $x = 0.25$, and quantum well width are very similar to the values reported in Ref. 8.

The blue line in Figure 1(b) shows the conductance G of the QPC at $B = 0$, demonstrating clear plateaux as a function of gate voltage V_g . The plateaux are a consequence of the 1D confinement in the QPC, where each occupied subband contributes $2e^2/h$ to the conductance. An in-plane magnetic field B_{\parallel} was applied parallel to the direction of transport in the QPC to induce Zeeman splitting. At $B_{\parallel} = 10$ T, the spin-degeneracy is lifted (red line in Fig. 1(b)) and the conductance is quantized in units e^2/h . The evolution of the spin splitting with applied magnetic field is shown in Fig. 1(a), where the transconductance dG/dV_g is plotted as a function of the gate voltage and magnetic field. The light regions mark the 1D subband edges, corresponding to the rises between conductance plateaux where dG/dV_g is maximum. The spin-splitting ΔE_z increases with applied magnetic field, which is observed as an increasingly large splitting δV_g between the bright regions in Fig. 1(a).

Unfortunately, the splitting ΔE_z cannot be obtained directly from Fig. 1(a), which only gives δV_g . To calculate the g -factor, it is necessary to convert δV_g into the subband energy scale, which is achieved by measuring the splitting in gate voltage due to an applied d.c. source-drain bias V_{sd} . We do this using the method developed by Patel *et al.*¹⁰ that combines measurements of the splitting due to the field $\delta V_g/\delta B_{\parallel}$ (Fig. 1(a)) with measurements of the splitting due to the source-drain bias $\delta V_g/\delta V_{sd}$ to give the absolute value of the g -factor:

$$|g^*| = \frac{1}{\mu_B} \frac{d(\Delta E_z)}{dB_{\parallel}} = \frac{1}{\mu_B} \frac{d(\Delta E_z)}{dV_g} \frac{dV_g}{dB_{\parallel}} = \frac{e}{\mu_B} \frac{\delta V_{sd}}{\delta V_g} \frac{\delta V_g}{\delta B_{\parallel}} \quad (1)$$

The source-drain bias measurements are shown in Fig. 2, where the transconductance dG/dV_g is plotted as a function of V_g and V_{sd} at $B_{\parallel} = 0$ (data have been corrected for

the d.c. bias dropped across the series resistance). Similar to Fig. 1(a), the light regions correspond to the transitions between 1D subbands (large dG/dV_g), marking the 1D subband edges. As the applied bias V_{sd} is increased, the subband transitions (light regions) split in gate voltage by δV_g , and conductance plateaux at half-integer $2e^2/h$ appear between the split transitions.^{16,17} Since the splitting δV_g is directly proportional to eV_{sd} , the energy scales associated with δV_g in Fig. 2 are obtained by calculating $e\delta V_{sd}/\delta V_g$.^{16,17}

The transconductance maxima in Fig. 2 cross when the applied source-drain bias is equal to the subband spacing: $\Delta E_{n,n+1} = eV_{sd}$,^{16,17} allowing the subband spacing to be directly extracted from Fig. 2. Values of $\Delta E_{n,n+1}$ calculated from these crossing points are listed in Table I and exceed 10 meV. The subband spacings are consistent with those obtained using magnetic depopulation measurements,¹⁵ and are double the spacings measured for etched $\text{In}_{0.47}\text{Ga}_{0.53}\text{As}$ quantum wires with InAlAs barriers.¹⁸ In Refs. 16 and 17 the ‘0.7 feature’ evolves into plateaux with $G \simeq 0.85(2e^2/h)$ at finite source-drain bias. In Fig. 2, we observe similar ‘shoulder’ plateaux with $G \simeq 0.8(2e^2/h)$, despite there being no clear 0.7 feature at $V_{sd} = 0$. Oscillatory structure is also observed on the conductance plateaux in Fig. 2, which has recently been linked to standing waves in the QPC¹⁹ and will be discussed elsewhere.

The Zeeman energies ΔE_z and g -factors are calculated using Equation (1) and the data extracted from Figs. 1 and 2. The splitting rates $\delta V_g/\delta B_{\parallel}$ and $e\delta V_{sd}/\delta V_g$ are listed in Table I. The Zeeman splitting of the 1D subbands ΔE_z is plotted against B_{\parallel} in the inset of Fig. 3, demonstrating a linear relationship for $B_{\parallel} \gtrsim 3$ T where the subband transitions are clearly resolved. Although the linear fits for the first two subbands do not extrapolate to zero at $B_{\parallel} = 0$ (due to the presence of the 0.7 feature and its analog at 1.7), still the g -factor can be extracted for each subband using Eq. (1).^{10,11} The values of $|g^*|$ are plotted as a function of n in Fig. 3. For the $n = 2$ and $n = 3$ subbands, we find that $|g^*|$ falls within the range previously reported for 2D $\text{Ga}_x\text{In}_{1-x}\text{As}$ systems.^{5,6,7,8} However, in contrast with Ref. 8, we obtain $|g^*| = 5.8 \pm 0.6$ for $n = 1$, confirming the presence of a 1D enhancement in our $\text{Ga}_{0.25}\text{In}_{0.75}\text{As}$ QPC.

In Ref. 8, the Zeeman splitting was measured with fields $3 \text{ T} \leq B_{\perp} \leq 8 \text{ T}$ applied perpendicular, rather than parallel, to the quantum well. This produces magnetic confinement due to Landau quantization that adds to the QPC’s electrostatic confinement. Ref. 8 reports 1D subband spacings that are smaller than the Landau level spacing for these fields.⁸ This is a non-physical result, since the addition of 1D confinement to a 2D system in a

perpendicular field cannot *decrease* the energy level spacing. For example, the 1D subband spacing is reported to be only 8.4 meV at $B_{\perp} = 4$ T when the 2D Landau level spacing is already 11.9 meV.⁸ Thus we suggest that the value of $|g^*|$ reported in Ref. 8 has been underestimated, which explains why no enhancement was observed. In contrast, our data are obtained with an in-plane magnetic field in the absence of Landau quantization. Our measurements show an enhancement of the g -factor as the QPC becomes more one-dimensional in agreement with previous results in 1D GaAs systems.^{10,11,12,13}

In summary, we have demonstrated that 1D confinement in a narrow-gap semiconductor such as GaInAs can result in a significant enhancement of the Zeeman splitting. Although the enhancement in $|g^*|$ is consistent with the trend observed in GaAs QPCs,^{10,11,12,13} the magnitude of $|g^*|$ measured for GaInAs QPCs is six times greater. Additionally, the subband spacing in our devices is quite large.¹⁵ Combined, the large g -factors and subband spacings found in etched GaInAs QPCs make them suitable for applications requiring spin-sensitivity at higher temperatures and with small magnetic fields.

We acknowledge financial support by the Australian Research Council, the National Science Foundation, and the Research Corporation.

-
- * Electronic address: tmartin@phys.unsw.edu.au
- † Department of Physics and Astronomy, University of Canterbury, Christchurch 8140, New Zealand
- ¹ S. A. Wolf, D. D. Awschalom, R. A. Buhrman, J. M. Daughton, S. von Molnar, M. L. Roukes, A. Y. Chtchelkanova, and D. M. Treger, *Science* **294**, 1488 (2001).
- ² J. M. Elzerman, R. Hanson, L. H. W. van Beveren, B. Witkamp, L. M. K. Vandersypen, and L. P. Kouwenhoven, *Nature* **430**, 431 (2004).
- ³ N. J. Craig, J. M. Taylor, E. A. Lester, C. M. Marcus, M. P. Hanson, and A. C. Gossard, *Science* **304**, 565 (2004).
- ⁴ N. Tombros, S. J. van der Molen, and B. J. van Wees, *Phys. Rev. B* **73**, 233403 (2006).
- ⁵ D. L. Vehse, S. G. Hummel, H. M. Cox, F. DeRosa, and S. J. Allen, *Phys. Rev. B* **33**, 5862 (1986).
- ⁶ M. Dobers, J. P. Vieren, Y. Guldner, P. Bove, F. Omnes, and M. Razeghi, *Phys. Rev. B* **40**, 8075 (1989).
- ⁷ I. G. Savel'ev, A. M. Kreshchuk, S. V. Novikov, A. Y. Shik, G. Remenyi, G. Kovács, B. Pödör, and G. Gombos, *J. Phys.: Condens. Matter* **8**, 9025 (1996).
- ⁸ T. Schäpers, V. A. Guzenko, and H. Hardtdegen, *Appl. Phys. Lett.* **90**, 122107 (2007).
- ⁹ M. Dobers, K. von Klitzing, and G. Weimann, *Phys. Rev. B* **38**, 5453 (1988).
- ¹⁰ N. K. Patel, J. T. Nicholls, L. Martín-Moreno, M. Pepper, J. E. F. Frost, D. A. Ritchie, and G. A. C. Jones, *Phys. Rev. B* **44**, 10973 (1991).
- ¹¹ K. J. Thomas, J. T. Nicholls, M. Y. Simmons, M. Pepper, D. R. Mace, and D. A. Ritchie, *Phys. Rev. Lett.* **77**, 135 (1996).
- ¹² A. J. Daneshvar, C. J. B. Ford, A. R. Hamilton, M. Y. Simmons, M. Pepper, and D. A. Ritchie, *Phys. Rev. B* **55**, R13409 (1997).
- ¹³ R. Danneau, O. Klochan, W. R. Clarke, L. H. Ho, A. P. Micolich, M. Y. Simmons, A. R. Hamilton, M. Pepper, D. A. Ritchie, and U. Zülicke, *Phys. Rev. Lett.* **97**, 026403 (2006).
- ¹⁴ P. Ramvall, N. Carlsson, I. Maximov, P. Omling, L. Samuelson, W. Seifert, Q. Wang, and S. Lourduoss, *Appl. Phys. Lett.* **71**, 918 (1997).
- ¹⁵ T. P. Martin, C. A. Marlow, L. Samuelson, A. R. Hamilton, H. Linke, and R. P. Taylor, *Phys.*

Rev. B **77**, 103811 (2008).

¹⁶ N. K. Patel, J. T. Nicholls, L. Martín-Moreno, M. Pepper, J. E. F. Frost, D. A. Ritchie, and G. A. C. Jones, Phys. Rev. B **44**, 13549 (1991).

¹⁷ A. Kristensen, H. Bruus, A. E. Hansen, J. B. Jensen, P. E. Lindelof, C. J. Marckmann, J. Nygård, C. B. Sørensen, F. Beuscher, A. Forchel, et al., Phys. Rev. B **62**, 10950 (2000).

¹⁸ T. Sugaya, M. Ogura, Y. Sugiyama, T. Shimizu, K. Yonei, K. Y. Jang, J. P. Bird, and D. K. Ferry, Appl. Phys. Lett. **79**, 371 (2001).

¹⁹ P. E. Lindelof and M. Aagesen, J. Phys.: Condens. Matter **20**, 164207 (2008).

TABLE I: Subband-dependent parameters of the QPC: subband spacing $\Delta E_{n,n+1}$, subband splitting rates $\delta V_g/\delta B_{\parallel}$ and $e\delta V_{sd}/\delta V_g$, and effective Landé g -factor $|g^*|$.

Parameter	$n = 1$	$n = 2$	$n = 3$
$\Delta E_{n,n+1}$ (meV)	13.1 ± 0.5	11.1 ± 0.5	9.9 ± 0.5
$\delta V_g/\delta B_{\parallel}$ (V/T)	0.029 ± 0.003	0.0371 ± 0.0015	0.0500 ± 0.0015
$e\delta V_{sd}/\delta V_g$ (meV/V)	11.6 ± 0.6	6.4 ± 0.3	4.4 ± 0.2
$ g^* $ - -	5.8 ± 0.6	4.1 ± 0.3	3.8 ± 0.2

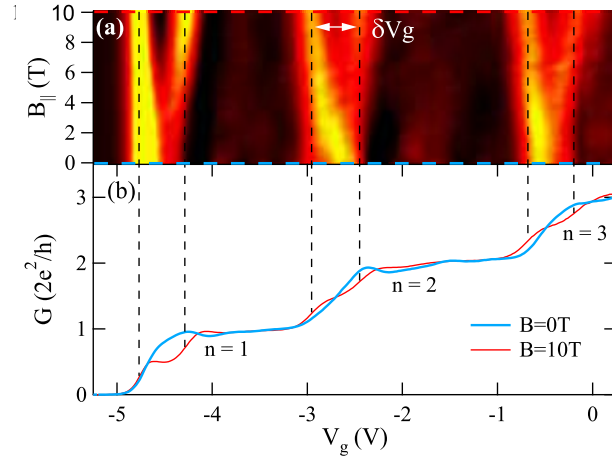


FIG. 1: (Color online) Zeeman splitting for the first three subbands of the QPC. (a) Transconductance dG/dV_g as a function of gate voltage V_g (horizontal axis) and magnetic field $B_{||}$ (vertical axis). Regions of yellow and red correspond to a large amplitude of dG/dV_g , indicating the locations of subband transitions. (b) Conductance G vs gate voltage V_g for $B_{||} = 0$ T (thick blue line) and 10 T (thin red line). Dashed lines in (a) indicate the region of the plot corresponding to the colored traces in (b).

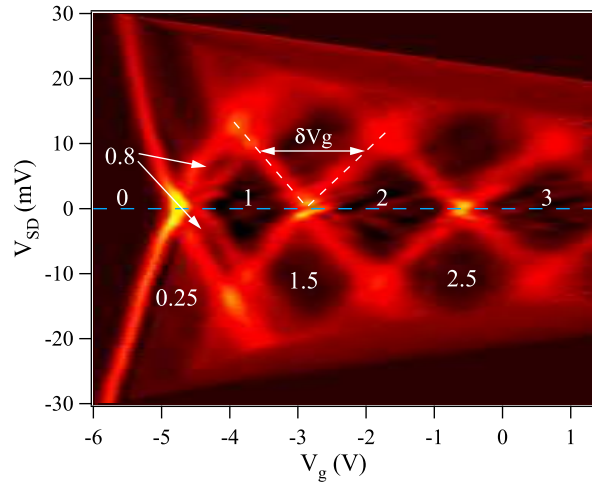


FIG. 2: (Color online) Transconductance dG/dV_g plotted as a function of gate voltage V_g (horizontal axis) and source-drain bias V_{sd} (vertical axis) at $B_{\parallel} = 0$. Regions of yellow and red correspond to a large amplitude of dG/dV_g , indicating the locations of subband transitions. The conductance G is labeled on each plateau in units of $2e^2/h$. Arrows indicate the $G \simeq 0.8(2e^2/h)$ plateaux that are linked to the 0.7 feature.^{16,17} The blue dashed line indicates the region of the plot that is equivalent to the blue trace in Fig. 1(b).

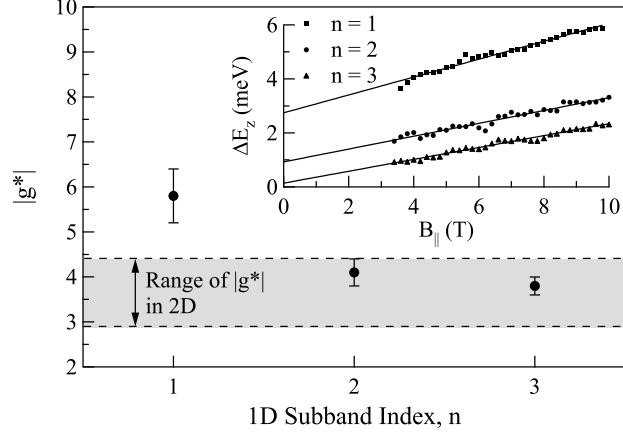


FIG. 3: Effective Landé g -factor $|g^*|$ in the QPC as a function of 1D subband index n . Dashed lines bound the range of $|g^*|$ previously measured for 2D $\text{Ga}_x\text{In}_{1-x}\text{As}$ systems.^{5,6,7,8} Inset: Zeeman splitting ΔE_z plotted vs magnetic field $B_{||}$. Linear fits are calculated between $3 \text{ T} < B_{||} \leq 10 \text{ T}$ and are then extrapolated to $B_{||} = 0$.